

# COMPOSITE COMPONENTS UNDER IMPACT LOAD AND EFFECTS OF DEFECTS ON THE LOADING CAPACITY

By

R. Aoki and D. Wurzel

(NASA-TM-75351) COMPOSITE COMPONENTS UNDER IMPACT LOAD AND EFFECTS OF DEFECTS ON THE LOADING CAPACITY (National Aeronautics and Space Administration) 47 p HC A03/MF A01 CSCL 11

NR0-16104

Unclassified  
47077

Translation of "Composite-Bautseile unter Schlagbelastung und Auswirkung von Defekten auf die Belastbarkeit," Deutsche Gesellschaft für Luft- und Raumfahrt, Symposium über Ermüdungsfestigkeit von Flugzeugen und modernen Bauweisen, Darmstadt, West Germany, Sept. 22, 1978, DGLR Paper 78-190, pp 1-48



NATIONAL AERONAUTICS AND SPACE ADMINISTRATION  
WASHINGTON, D. C. 20546 SEPTEMBER 1979

## STANDARD TITLE PAGE

1. Report No. NASA-TM-75351	2. Government Accession No.	3. Recipient's Catalog No.	
4. Title and Subtitle  COMPOSITE COMPONENTS UNDER IMPACT LOAD AND EFFECTS OF DEFECTS ON THE LOADING CAPACITY		5. Report Date September 1979	6. Performing Organization Code
7. Author(s) R. Aoki and D. Wurzel German Institute for Aeronautical and Astronautical Research and Development		8. Performing Organization Report No.	10. Work Unit No.
9. Performing Organization Name and Address Leo Kanner Associates Redwood City, California 94063		11. Contract or Grant No. NASW-3199	13. Type of Report and Period Covered Translation
12. Sponsoring Agency Name and Address National Aeronautics and Space Administration Washington, D.C. 20546		14. Sponsoring Agency Code	
15. Supplementary Notes Translation of "Composite-Bauteile unter Schlagbelastung und Auswirkung von Defekten auf die Belastbarkeit." Deutsche Gesellschaft für Luft- und Raumfahrt, Symposium über Ermüdungsfestigkeit von Flugzeugen und modernen Bauweisen, Darmstadt, West Germany, Sept. 22, 1978, paper 78-190, 48 pages (A79-20491)			
16. Abstract Investigations were carried out on the development of a horizontal tail assembly made of carbon fiber reinforced plastic for the Alpha Jet. Possibility of obtaining a leading edge nose design lighter but not more expensive than a metal version was studied. Important consideration was sufficient resistance of the leading edge against impact of stones and hailstones combined with high degree of stiffness. A survey of development work to improve energy reception characteristics of the material through suitable laminate design is provided. Design is usually based on characteristics of parts made of undamaged fiber reinforced laminates. Since certain defects will occur in structural components, the effects of such defects on the characteristics of the parts was also studied			
17. Key Words (Selected by Author(s))		18. Distribution Statement Unclassified-Unlimited	
19. Security Classif. (of this report) Unclassified	20. Security Classif. (of this page) Unclassified	21. No. of Pages 47	22. Price

COMPOSITE COMPONENTS UNDER IMPACT LOAD AND EFFECTS  
OF DEFECTS ON THE LOADING CAPACITY

By

R. Aoki and D. Wurzel  
DFVLR, FBWB--BK Stuttgart

DGLR Symposium  
"Fatigue Strength of Airplanes and Modern  
Construction Techniques"

Darmstadt, September 22, 1978  
Paper No. 78-190

D F V L R

COMPOSITE COMPONENTS UNDER IMPACT LOAD AND EFFECTS  
OF DEFECTS ON THE LOADING CAPACITY

Contents:	Page
Part A: Dipl. Ing. D. Wurzel Composite Components Under Impact Load	4
Part B: Dipl. Ing. R. Aoki Effects of Defects on the Loading Capacity of Composite Materials	17

Table of Contents

	Page
Part A - D. Wurzel	5
1. Introduction	
2. Preliminary Investigations of Impact Resistance	
3. Structural Design of the Nose and Selection of Material	
4. Simulation of Damage From Stones and Hailstones	
5. Damage From Stones and Hailstones	
5.1 Expanded Investigation of Damage From Natural Stones	
5.2 Other Impact Stresses	
6. Effects of Damage From Stones and Hailstones on Operational Behavior	
7. Summary	
Part B - R. Aoki	17
1. Introduction	
2. Test Program	
3. Failure of Strip Samples Made of GFK Due to Surface Damage	
4. Failure of Strip Samples Made of CFK Due to Surface Damage	
5. Summary	

## Abstract

### Part A

#### Composite Components Under Impact Load

A requirement existed for the development of a design concept for a tail assembly nose made of composite fibers and to prove its operational efficiency through tests on part sections. In addition to the requirement for low weight and low costs, high rigidity and impact resistance were called for. A suitable laminate construction with high energy absorption capacity had to be found for that.

In an experimental program the effects of damage, particularly through stones and hailstones, on the operational behavior of composite noses was investigated. The suitability of composite fiber materials could be confirmed for the projected purpose.

### Part B

#### Effects of Defects on the Load Capacity of Composite Materials

The behavior under varying tensile stress, of undamaged sample strips made of GFK and CFK and those damaged through impact by a starpunch, is investigated as part of an ongoing program on defects in FVW and their effects by the Institute for Methods of Construction and Design Research of the DFVLR.

The influence of the stress level on the type of failure of various damaged samples made from GFK and CFK is shown, the influence on the residual strength of CFK samples after a test applying variable tensile stress, is determined.

## 1. Introduction

/1\*

The Institute for Methods of Construction and Design Research is occupied, among other things, with the design and development of a tail assembly nose as composite structure including experimental proof of its operational behavior from nose sections in life-size dimensions; all of this being carried on within the scope of a development, sponsored by the Dornier Co. as part of the KEL program, for a CFK horizontal tail assembly of the Alpha-Jet. The desired result is a nose that will be lighter, but under no condition more expensive, than the metal version. The structural design was determined from a finite-element calculation offering three alternatives, as a skin and ribs construction primarily because of the requirement for rigidity.

One important mechanical requirement for the composite nose is sufficient resistance capability against damage from stones and hailstones. Behavior during stress through impact and shock is one of the critical characteristics of fiber-reinforced materials, particularly when high rigidity is required in addition to high impact resistance. Such requirements cannot be met by a fiber material alone but can be achieved by combination of a rigid fiber material with an impact resistant fiber material into a hybrid material.

The following contribution offers a survey of the work that we carried out for improvement of energy absorption by suitable buildup of laminates. High reversible energy absorption, high energy consumption in failure and small damage areas were aimed for.

---

\*Numbers in the margin indicate pagination in the foreign text.

The basic investigations into the impact behavior of the composite materials were started with an instrumented pendulum impact testing machine, on samples of the materials, not to obtain dimensional characteristics but for estimation of the magnitude of influences of varied angular arrangements, mixture ratios and laminate buildups. The bombardment of flat plates at first made it clear that fabrics have higher impact resistance than unidirectional layers which tend towards easier splitting. Consideration of the requirements for rigidity led to determination of the principle of hybrid laminate buildup for the nose planking. The subsequent bombardment of part sections also showed the influence of curvature at the leading edge region of the nose. To keep the weight to a minimum, the configuration was planned to allow only small damage, as is the case for the metal version. /2

Suitable test procedures were developed to simulate damage from stones and hailstones under laboratory conditions. The bombarded noses are tested for effects of the damages on service life, in a comprehensive test program that is about to be concluded.

The requirement for a manufacturing method that would, in addition to sufficient impact resistance, also be cost-effective led, during the development of a suitable design concept for the tail assembly nose, to an expansion of the impact resistance investigations to nose sections from three different fiber/resin systems, which were produced according to different methods.

## 2. Preliminary Investigations of Impact Resistance

/3

Composites show characteristic differences in the way they fail under impact stress. That becomes particularly clear during three-point impact bend tests with an instrumented pendulum

impact testing machine where hammer force and path are automatically recorded. Fibers with high modules are usually brittle: CFK samples are cleanly penetrated after a maximum load is reached and energy absorption remains low. The residual pieces are hardly damaged, however, and can still be highly stressed. In GFK or Kevlar/Epoxy samples a lot of energy absorption occurs until failure starts. Energy is still absorbed, even after the maximum stress has been reached, with the laminate being destroyed over large surrounding areas. Unfortunately, such impact resistant fibers usually have a lower modulus of elasticity.

To meet the contrasting requirements for fiber materials with regard to high rigidity and impact resistance, simultaneously, a stiff type of fiber must be combined with one that absorbs energy into a hybrid material for the material of the nose covering. CFK and GFK were chosen as suitable basic materials. Kevlar/Epoxy was not yet considered as an alternative at this time because of its high sensitivity to humidity and its difficult machinability.

To combine the positive characteristics of CFK and GFK optimally in a hybrid material impact bend tests were carried out for various mixture ratios and layer arrangements. Fig. 1 shows the total energy absorbed during sample fracture for unidirectional glass/carbon hybrid laminates, as a function of the mixture ratio and the energy portion that can be absorbed without damage, i.e., reversibly. The impact resistance is clearly determined by the GFK portion. T300 and FT-hybrids are superior to the HM hybrid. /4

The influence of the layer arrangement was investigated for T300/E-glass hybrid samples by arranging the components alternately from layer to layer (alternating buildup) for various mixture ratios, resp. to combine the basic materials so that

one partner is arranged midway between the other (blocked build-up). The highest impact resistances are obtained for a blocked arrangement.

The highest total energy is consumed when the GFK is positioned in the middle, as per Fig. 2. Failure begins with the fracture of the carbon layers on the compression side of the sample. Much energy is still absorbed after maximum stress load has been reached because of the progressive bending fracture of the intermediate glass layers.

The highest reversible energy absorption for an appreciable total energy consumption is, however, reached through arrangement of the CFK in the middle. This arrangement close to the neutral plane decreases the bending stress of the carbon fibers. The elastic region is limited through cracks and shear fractures in the boundary region of the various fiber layers. An optional reversible absorption exists when the proportional volume of GFK is more than 60% of the total fiber volume. For proportions of GFK below that value a drastic decrease of energy absorption occurs. /5

During numerous individual tests through bombardments of flat plates it became clear that carbon textures have advantages over UD-layers with regard to damage propagation and damaged areas. Long fissures in the fiber direction, strip formation and excessive delamination areas occur at projectile impact even when unidirectional single layers have been arranged crosswise, one above the other. These fissure formations do not occur in fabrics because of their interlinkage; the stress is distributed over a larger part of the total structure and the local stresses are reduced that way.

### 3. Structural Design of the Nose and Selection of the Material

Based on the information gained from the preliminary investigations a blocked buildup of CFK and GFK fabrics, with the CFK part in the middle, was chosen for the nose covering, promising high energy absorption without damage, high energy consumption during failure and a small damage area, thus fulfilling all requirements.

Fig. 3 shows the version proposed for the CFK-horizontal tail assembly as example of the structural buildup of the nose. /6

The planking is formed by a hybrid buildup from continuous layers of CFK and GFK fabrics. All layers are oriented in a  $\pm 45^\circ$  direction to increase torsion resistance. The leading edge exposed to damage by stones and hailstones is protected by additional glass fiber layers. The juncture region is made more rigid with CFK since the crossforces resulting from air pressures can only be disposed of via the planking, so as to permit a detachable connection required for inspection and maintenance reasons. Deformations due to those crossforces are controlled by CFK ribs as well as by the juncture reinforcement.

Work on the process technology for optimization of the nose fabrication with regard to costs and weight determined that experimental nose pieces would be made of three different fiber/resin systems.

The system used first was Code 69, a  $175^\circ\text{C}$  high pressure, high-bleed system and the basic material for the CFK-spar box; it had to be discarded because of the strong resin flow. The transition to a  $120^\circ\text{C}$  low pressure, low-bleed system was carried out at first with Fibredux 920. But since no CFK fabric could be supplied in sufficient quantity a second low pressure material,

system Vicotex 145? which was immediately available, was included in the tests. The results obtained with it led to the qualification of this system for the building of a prototype.

Knowledge gained in manufacturing technology during the processing of these three systems and results obtained from the impact tests permitted a step-by-step simplification of the design. /7

In addition to the conventional manufacture of planking and ribs in separate autoclave operations with subsequent gluing, manufacture of skin and ribs in one operation succeeded for the first time with the Vicotex system, by means of a pressure bag. The saving in operational steps and the elimination of tolerance problems connected with it, makes possible a reduction of manufacturing costs. This "pressure bag method" is therefore to be applied for the building of prototypes.

#### 4. Simulation of Damage From Stones and Hailstones

Impact damage to the nose is caused during takeoff and landing by stones propelled upwards from the runway and during flight by hailstones. To prove that composite noses exposed to such impact stresses are not influenced detrimentally any more than conventional aluminum noses, test arrangements were set up for simulation of damage from stones and hailstones in the laboratory. Bullets of glass and ice were used instead of stones and hailstones, since they were easily obtainable, to establish reproducible test conditions. For a given velocity (about 50 m/s corresponding to takeoff and landing speeds) the mass of the glass spheres was determined so that dents of about 1 mm depth are produced under the same conditions on frontally bombarded, presently used, tail assembly noses made of sheet metal. Damages beyond that may not be tolerated according to maintenance /8

procedures and for aerodynamic reasons must be repaired or lead to an exchange of the nose. This boundary condition is reached with glass bullets of 13-14 g weight (dia.= 21.5 mm).

During bombardment of the aluminum tail assembly nose with ice bullets at about 250 m/s (near maximum flight velocity) no corresponding deformations occurred at the tip of the nose. Ice bullets disintegrate upon impact into sandcorn sized particles that can slide off the leading edge of the nose without causing major damage or any damage at all perhaps. The ice bullet diameter was therefore fixed at 15 mm (mass of about 1.6 g), a size corresponding to an average hailstone size.

The propulsion of the glass bullets was arranged through a high pressure cannon, the ice bullets were shot from a shotgun. In both cases the projectiles were imbedded in foam cartridges, see Fig. 4.

The glass bullets were shot directly against the leading edge of the nose sections to be tested. The ice bombardment occurred directly and at an angle of 20° to the direction of flight, against the nonreinforced side of the nose.

##### 5. Damage From Stones and Hailstones

19

During the simulation of stone impact no permanent deformations resulted in any of the test pieces. That part of the energy which was not absorbed through elastic deformation led to delaminations of varying sizes, dependent on the exact location of impact, impact velocity and impact angle (dispersion among bombardment parameters). The same bombardment conditions also produced, at the impact side of the laminate, similar delaminations up to 2 cm diameter. For the somewhat brittle Code-69 system the

delaminations were markedly greater on the backside of the laminate than in front, as per Fig. 5. For the two other systems damages were about equal on the backside, for Vicotex 1452 perhaps even smaller than in front, as per Fig. 6. In addition to the delaminations the laminates of this system, which are thinner than those in the other variations, also showed evidence of slight fissurelike damages in the GFK.

During ice bombardment of the leading edge of all versions, no damages occurred. For impact angles of  $20^\circ$  to the side, no damages were recorded as well. Even repeated hits on the same spots provided no different picture. Hailstones of the size used here will therefore not present any danger at frontal or angular impacts that are slightly inclined to the direction of flight, even during high flight velocity.

On the ground, damage can be wrought by a hailstorm through hailstones that impact at right angles to the surface of the top side of the nose and may do harm. For that reason, several experimental pieces were bombarded at right angle to the surface with ice, the experimental velocity again being 250 m/s. The laminate was therefore stressed far beyond conditions in real life. For the Code-69 system--brittle, as mentioned before--a slight delamination on the side of the impact was opposed by a delamination nearly the size of a hand on the backside. In the Vicotex system only small damage with regard to area size occurred, even under these unfavorable conditions. In addition it should be pointed out that under the same conditions a dent of about 40 mm diameter was caused in the metal nose, with a depth of several millimeters.

/10

During the design layout of the nose, care must be taken that the ribs not reach right up to the leading edge which is particularly exposed to impacts since the resulting stiffness of

that region would restrict the amount of energy that could be absorbed reversibly, particularly in case of frontal stone impact.

### 5.1 Expanded Investigation of Damage From Natural Stones

To round out the picture, but giving up reproducibility in this instance, the original metal nose and the nose sections built up according to the proposal for the CFK-tail assembly, were bombarded with real stones, as per Fig. 7a. For that purpose pebbles, as they are used for concrete aggregates, were chosen along with some sharp-edged ones.

The respective masses were between 6 and 12 grams, an order of magnitude that can easily get on a runway. /11

Compared to the heavy glass bullets damage caused by pebbles impacts basically less, as might be expected. During propulsio of a whole series of sharp-edged stones it happened only once that a stone impacted with the sharp edge in front. In that case the outer glass layer was involved, as per Fig. 7b.

For reasons of surface quality (lacquer damages) this may require repairs. But bombardment of the sheet metal nose showed that similar hits in this case would also not be tolerated without repairs.

### 5.2 Other Impact Stresses

In addition to endangerment through stones and hail storms, which concern primarily the leading edge of the nose, the nose structure can also be exposed to other impact dangers, particularly on the ground, during servicing and maintenance of the airplane. Collision with obstacles or dropped tools can be envisioned.

The effects of a dropped tool were investigated through tests with the fall of a screwdriver weighing 115 grams. It was dropped from a height of 1.8 m on composite nose sections as well as on the sheet metal nose, with the blade forward. The planking made of composite fiber structure was shown to be superior: a light spot of about 1 mm diameter and a small notch indicated the impact location; there were no traces on the backside of the laminate, as shown in Fig. 7c. The metal planking showed a marked dent, however, with a crack in the backside of the sheet metal. /12

#### 6. Effects of Damage From Stones and Hailstones on Operational Behavior

Stressing of the nose box in flight occurs through local distribution of lift as well as through flexure and torsion of the entire structure, which is determined by the sparbox.

Determination of the effects of damage from stones and hailstorms on the operational behavior of noses structured from hybrid composites was carried out in two series of experiments in which air pressure flexure and bending-torsion were simulated. The highly simplified experimental stresses were so applied that the same or greater deformations occurred in the impact region, as would be expected from theoretical calculations of air pressures at the horizontal tail assembly.

Fig. 8a shows the experimental buildup for testing the deformations under air pressure. The level of stress was at that of the design stress divided by 1.5. A second test stand was used for creating torsion with superimposed flexure, as shown in Fig. 8. The torsion angle exceeded the calculated one considerably in this case (about  $0.3^\circ/m$  against  $2.7^\circ/m$ ).

The nose sections that had not been bombarded were at first exposed to about 20,000 stress cycles ( $f=2$  Hz) in the two experimental installations, with all deformations and forces being recorded as basic values. After bombardment the stress test was continued with at least 40,000 stress cycles, in some cases up to 120,000 stress cycles. Deformations and forces were again recorded and compared with those before the bombardment, resp. checked for changes during the test procedure. /13

For nose section of the design planned for the prototypes the air pressure deformation program ended with a static fracture test.

After completed bombardment no detrimental effect on the load capacity of the noses could be proven from these single phase stress experiments. There was neither an enlargement of the visually noticeable damage areas nor could changes be recorded in the test values, after the bombardment damage of the planking had taken place, which would lead to conclusions about changes in the damage areas during the course of the test.

With the proposal of a design for a composite nose of the CFK-horizontal tail assembly the basic experiments have been more or less concluded. A few more specific observations are planned of the effects of hits in the region of the glued in, resp. laminated in, ribs to determine if and how the connection between rib and skin, and the rib flange, can be affected. In the proposed layout of the tail assembly nose the ribs do not reach immediately up to the particularly impact-exposed tip of the nose, but take up a region that is endangered only by glancing hits or by hits at a very obtuse angle. /14

Experiments with ultrasound were carried out by the Dornier Co. on several nose pieces, to determine whether additional

damages beyond those visible were present in the bombarded noses. Up to now no useful results have been achieved. The experiments are being continued.

The investigations into process technology are being concluded with studies on the refinement of the pressure bag procedure.

#### 7. Summary

The goal of the investigation was to develop a tail assembly nose of composite fiber design and to prove its suitability for the proposed application. Of particular interest was the degree of resistance to impact stresses by stones and hail that could be achieved while maintaining a design that met the requirements of low weight, high strength and high rigidity. Test installations were set up in which conditions of stone and hail impact could be simulated. In an experimental program nose sections made of various fiber/resin systems and built-up layers were bombarded and the effects of the damages investigated with respect to the operational behavior of the composite noses. Based on the available experimental results the detrimental effect on the stress capacity of the nose is small after bombardment, if not entirely insignificant. No changes could be recorded in this connection among damages or test values. This proves that the attempted compromise of tolerating light damage, particularly delaminations, for the sake of maintaining low weight, permits solutions that are impact resistant and therefore useful. Since practically no plastic deformations occurred in the region of the leading edge, there is far less detriment as consequence of impact damage than in the case of the conventional metal version, from the aerodynamic point of view. /15

Weight savings of almost 20%, compared to the present metal model version, are possible for the lightest one of the noses investigated, while maintaining sufficient impact resistance, as shown in Fig. 9. This version was proposed for use in the CFK-horizontal tail assembly of the Alpha-Jet.

The investigations of this contribution dealt only with the impact behavior of an actual part of composite fiber design. It was tested and the determination was made that the occurring impact damages had no negative effect on its stress capacity and operational behavior. A separate program was started for a general investigation of the effects of impact damages to the microstructure of composite fiber materials.

Part B

/16

Effect of Defects on the Load Capacity of Composite Materials

1. Introduction

/17

In the design of parts made from fiber reinforced materials one usually starts with undamaged laminates. Otherwise it is hardly avoidable to get parts that contain defects, i.e., faults or damages. This requires some judgment, independent of the respective cause of damage, on how the effect will influence the operational stress capacity.

Defects in FVW and their effects were investigated, among others, at our Institute. Following is a report about some of the results.

The various phases of a composite part are sketched roughly in Fig. 10. This shows in which phases defects can occur. The structural-strength model, as well as the defect model for fiber

reinforced materials, are still in the definition phase. For a defect-model it is necessary to know: when, where and how, i.e., the event, the location and the way in which the defects occur and what their effects are with respect to the stress capacity of laminates or of composite parts.

Looking first at the event, a tabulation can be made in which the causes can be mechanical, thermal, chemical, human or a combination of these facts (see Fig. 11). In a classification according to the damage location, defects on the surface, in the laminate layer proper, or between the laminates, can occur or extend over the whole laminate. When classifying according to the type of damage, differentiation can be made between fiber-specific, resp. matrix-specific damages, such as differences in the fiber strength, fiber breaks during manufacture, wrong mixture ratio during resin application, or delaminations, foreign bodies and air bubbles that may appear singly or in combination.

The effects of the defects on the stress capacity of laminates or composite parts are dependent on the one hand on the already mentioned factors, on the other on the type of stresses, resp. combinations, to which the laminates are subjected at the moment the damage occurs and afterwards, as well as on the environmental conditions to which they are exposed. /18

Here are a few examples as explanation:

The impact of a stone (mechanical cause) can, dependent on the mass, angle of incidence, shape of the body, consistency and relative velocity to the part, cause a crack, a scratch or a partial fracture on the surface. Fiber/matrix damages or, eventually, a local delamination can occur in the intermediate layer in this case. The number of laminate layers may be wrong due to

carelessness in fabrication (human cause during fabrication). The effects would be recognizable in the strength characteristics of the laminate.

## 2. Test Program

/19

The number of possible defects that can occur in composite parts is very large. It must be expected that they are statistically significant. Damages that actually occur do provide information about failures to be expected, but they are less suitable for reproducible evidence about failure progress and service life. For that reason we decided at first to simulate defects of a mechanical nature in the laboratory.

The investigations will extend to real, simulated and idealized defects and, not the least, to defect free samples, as shown in Fig. 12.

By a real defect we understand such damages as may occur during operation. The simulated defect is produced with laboratory tools so that it corresponds in its characteristics to a real damage. It has the advantage that it can be reproduced. The idealized defect must on the one hand possess the comparable characteristics of an actual damage tree, but on the other hand it must be geometrically so simple as to permit analytical treatment of the damaged sample. Such an idealization of bombardment damage could be a hole drilled in steps, for instance.

The test samples are produced for the most part from prepreg material by the autoclave method. They can be built up from fabric, unidirectional or multidirectional layers or their combinations. The samples are subjected to static, resp. dynamic, tension, compression, bending and buckling tests.

The factors to be investigated are, among others: permissible number of stress cycles at a certain stress level, decrease in stiffness, mechanism of damage propagation, residual strength, failure mode as a function of the stress level, the influence of the laminate buildup and the mean time before failure forecast.

The results from investigations of these parameters have direct importance for the safety and utility of composite parts. /20

During the first phase of our program we restricted ourselves to undamaged samples and those samples in the form of strips and plates, which were damaged through simulated defects, all of them made of GFK and CFK.

At present we are investigating the effects of two simulated types of defects:

1. The bombardment test with a glass bullet (Fig. 12).
2. Generation of a defect through a punch mark.

Following is the report on the investigation of strip samples, which were damaged with a pressure punch at the surface under reproducible conditions. Subsequently, static and dynamic stress tests were carried out in an hydraulic testing machine.

### 3. Failure of Strip Samples Made of GKF Due to Surface Damage

/20

The tests were first carried out with GFK-samples since their transparency permits better observation of the propagation of damage.

The first tests were made with test samples having surface damages that could be reproduced faithfully through impression of

a spherical, resp., starshaped pressure punch. Such damages can occur on the skin of a composite wing due to the fall of a tool or the impact of a stone. The damages (damaged surface:spherical impression  $\approx 30 \text{ mm}^2$ , star impression  $\approx 90 \text{ mm}^2$ ) were produced with a punch force of 5 kN in each case, with the sample resting on a rigid base.

The layers close to the surface show additional delaminations in this case. The impression of the sphere, resp. star, amounts to 10  $\mu\text{m}$ , resp. 20  $\mu\text{m}$ . The GFK (glass fabric 181/Code 69, 0/90) strip samples (250 x 35 x 2 mm) were subjected to static and dynamic tensile stresses ( $t = 20^\circ\text{C}$ ,  $f = 2.5 \text{ Hz}$ ). Fig. 13 gives information about the behavior of such damaged laminates during tensile stresses of varying magnitude. While the influence of these impressions on the vibration stress is not very pronounced the failure mode is strongly influenced by the chosen stress level.

Delamination cores appear at the intersections of the glass fabrics which spread increasingly over the entire sample, when the stresses become high on the undamaged samples as well as on those with spherical and star-shaped damages (Fig. 14).

In samples with a star-shaped damage an additional laminar delamination occurs, which spreads quickly from the damage location (Fig. 14 bottom). At high stresses undamaged samples fail similarly to those with spherical damage, but samples with star-shaped damage fail from the location of the damage outwards.

At low stresses all samples fail, after initial transverse fissure propagation, through separation fracture. At this stress level no difference can be observed therefore in the failure modes of undamaged or damaged samples (Fig. 15).

#### 4. Failure of Strip Samples Made of CFK Due to Surface Damage

/21

The CFK-strip samples were prepared in the autoclave from UD-prepregs (T300/CODE 69).

Sample	Composition	Dimensions
A	(0 <sub>2</sub> /±45/0 <sub>2</sub> /90) <sub>S</sub>	250 x 16 x 2.4 mm
B	(0/90) <sub>3S</sub>	250 x 16 x 1.7 mm

As with the GFK samples, the generation of the star-shaped damage (Fig. 16) is carried out by means of a punch, but with variations in the depth of penetration.

The influence of the damage parameters, pointed angle and punch force P, on the static tensile strength ( $\sigma_{st}$ ) is shown on hand of the example of the B-sample with star-shaped damage (Fig. 17).

The A and B samples were again stressed statically, resp. subjected to tensile stresses of varying magnitudes ( $t=20^\circ\text{C}$ ,  $f=5\text{ Hz}$ ).

The damage parameters for the majority of the tested samples are  $=160^\circ$  and  $P=5\text{ kN}$ . The penetration depth (ET) amounted to  $\sim 317\text{ }\mu\text{m}$  for the A-samples, resp.  $\sim 300\text{ }\mu\text{m}$  for the B-samples, the visibly damaged area measured  $\sim 12\text{ mm}^2$  for A-samples and  $\sim 9\text{ mm}^2$  for the B-samples.

Fig. 18 shows the results of static and dynamic investigations. The maximum stresses of the stress tests of varying magnitude are plotted as ordinate values with reference to the average static tensile strength of the undamaged sample, the stress cycle numbers to breaking stress are plotted in the abscissa.

The values on the ordinate ( $N=10^\circ$ ) show the relative static tensile strength of the damaged samples. The influence of the damage on the tensile strength is easily recognizable here. While the "slightly damaged" ( $ET \sim 10 \mu\text{m}$ ,  $\approx 130^\circ$ ,  $P=5 \text{ kN}$ ) A-samples offer higher strength values than the undamaged samples, a decrease of up to nearly 70% of the static tensile strength may be observed for samples with heavier damage ( $ET \sim 300 \mu\text{m}$ ,  $\approx 160^\circ$ ,  $P=5 \text{ kN}$ ).

The damaged B-samples ( $ET \sim 300 \mu\text{m}$ ,  $\approx 160^\circ$ ,  $P=5 \text{ kN}$ ) show lower values when compared to the A-samples, which may be a function of the difference in local penetration of the damage. The penetration depth of the punch amounted to  $\approx 13\%$  of the sample thickness for composition A and to  $\approx 20\%$  of the sample thickness for sample B. /23

The behavior of all tested CFK samples during stress tests of varying magnitude is characterized by a slight decrease of vibration strength with the increase in stress cycles.

The different failure mode of CFK samples tested during the stress test of varying magnitude is brought about by the different lamination buildup.

In all A-samples fiber breaks occurred first along the longitudinal edges. They were followed by fissures in the  $90^\circ$  layer, then by delamination near the fissure, later also partial fissures and delaminations between the  $45^\circ$  and  $0^\circ$  layers.

In the A-samples with star-shaped damage two longitudinal fissures appeared that ran parallel to one of the clamping directions, caused by the outer  $0^\circ$  layers. During further stressing of the sample that part of the  $0^\circ$  layer which is enclosed by the two longitudinal fissures delaminated completely.

For some samples it could be observed that the adjacent 45° layer was completely rubbed off in this delamination region. The failure set in through a separation fracture at the damage location.

Fiber breaks also occurred along the longitudinal edges in undamaged B-samples. Fissures in the 90° layers were not observed, however.

The B-samples with star-shaped damage behave similar to those that are undamaged. In contrast to the A-samples a partial delamination of the damaged surface layers could be observed only in a very few cases.

The failure of the probe then occurred through a sudden separation fracture at the damage location.

One criterion for the effect of defects on composite laminates and parts is their residual strength after dynamic stress. In Fig. 19 residual strengths obtained for undamaged and star-damaged A- and B-samples are plotted against the stress cycle number. Tensile stresses of varying magnitude were applied at different stress levels (see Fig. 20).

A few undamaged A-samples showed an increase in residual strength vs. tensile strength in spite of a high stress level for tensile stress tests of varying magnitude ( $\sigma_0/\sigma_{st} \approx 0.80$ ) and a large stress cycle number ( $\approx 10^6$ ).

No such behavior was observed for undamaged B-samples.

The residual strength values for A-samples with star-shaped damage are, independent of the stress level of the tensile stress of varying magnitude, higher after  $10^3$  stress cycles than the

tensile strength value of the A-samples with star-shaped damage. A- and B-samples with star-shaped damage show a decrease in residual strength after tensile stress tests at varying magnitude and high stress cycle numbers ( $N=10^6$ ). Fig. 20 shows the residual strength (relative to the tensile strength of the respective undamaged samples A, resp. B) as function of the maximum tension level of the tensile stress test of varying magnitude. Comparison of the values obtained for residual strength at various stress levels indicates that the maximum stress level influence on the tensile stress test of varying magnitude of tension appears to be small.

## 5. Summary

/25

Static tension, resp. dynamic behavior of GFK and CFK during tensile stress tests of varying magnitude of tension were investigated on undamaged strip samples and those damaged through surface impressions.

Some influence of the stress level on the failure mode could be observed for the GFK samples while such behavior could not be observed for CFK test samples.

The GFK samples that had been damaged through a star-shaped punch mark show a different failure mode than samples that were damaged under the same conditions by a spherically shaped punch.

Dependence of the tensile strength on the damage parameters and pressure force  $P$  of the star-shaped punch occurred in the damaged CFK test samples.

CFK test samples (damaged and undamaged) showed a slight decrease in vibration strength for increased stress cycle numbers.

The residual strength of damaged and undamaged CFK samples appears to be independent of the maximum stress level of the tensile stress test of varying magnitude. The available results point to the necessity for investigation of the effects of defects on FVK laminates.

Classification of the defects, which has been indicated here, was to be further refined into a defect matrix. This is the premise for the analytical treatment of actual damage trees and therefore for the setting up of a defect-model for a certain type of defect.

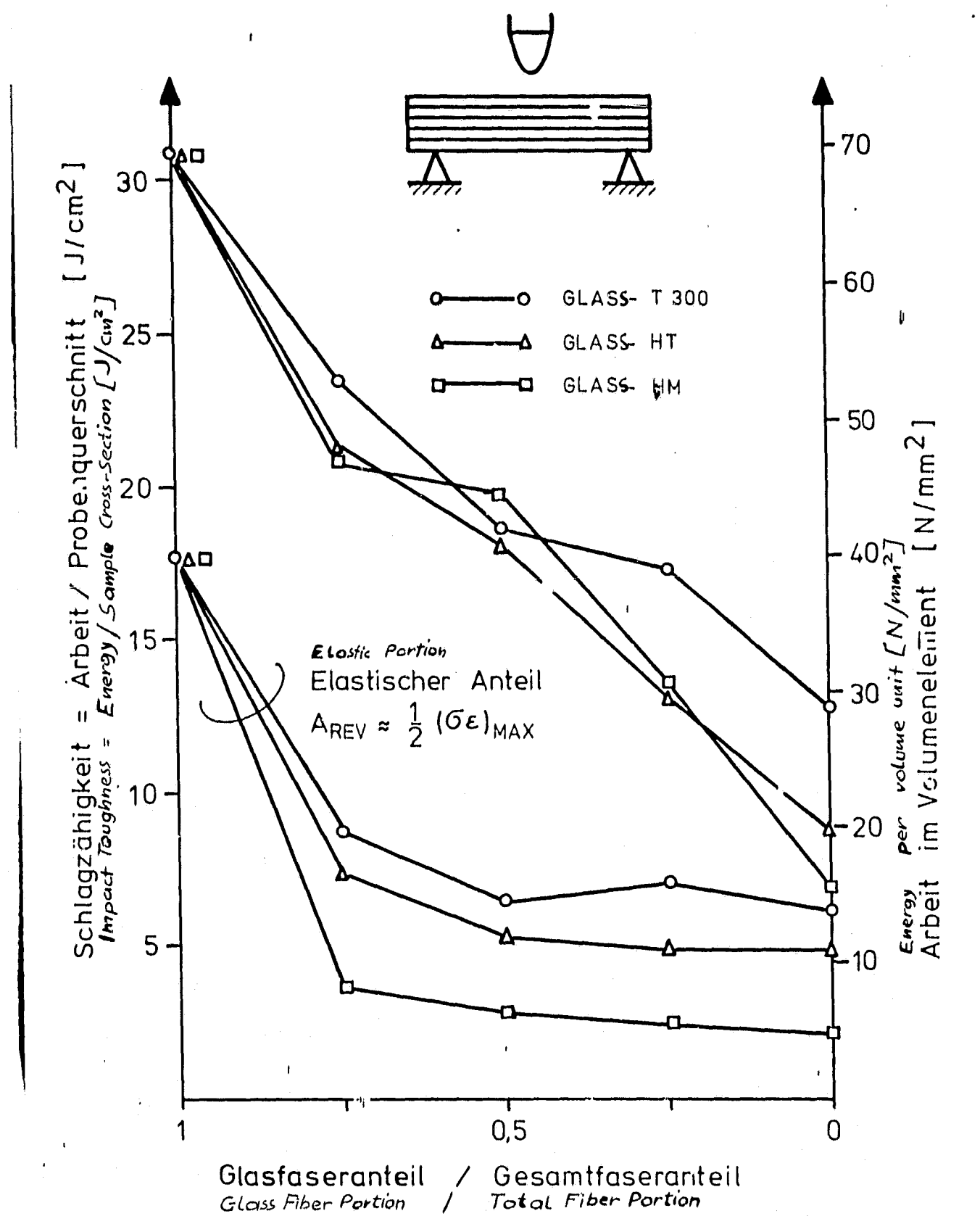


Fig. 1. Impact energy absorption and mixture ratio.

Blocked Buildup

Geblockter Aufbau

CFK/GFK/CFK

GFK/CFK/GFK

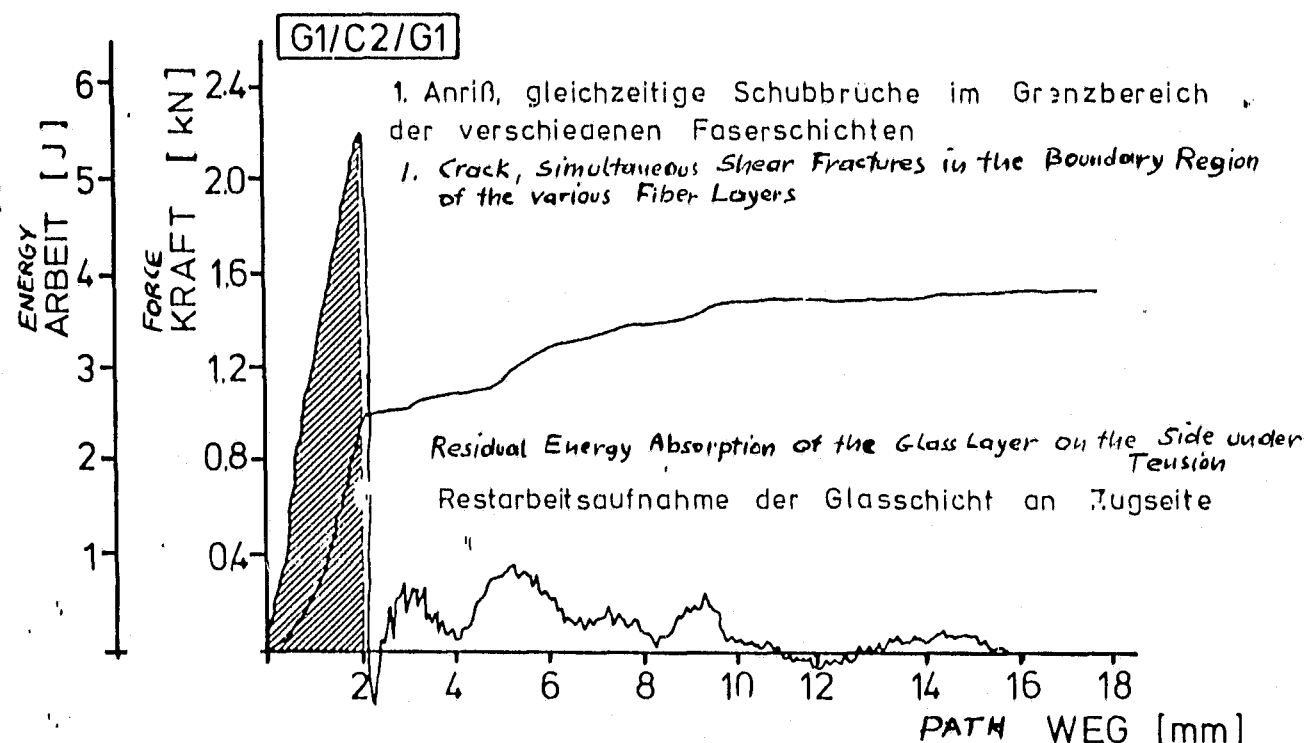
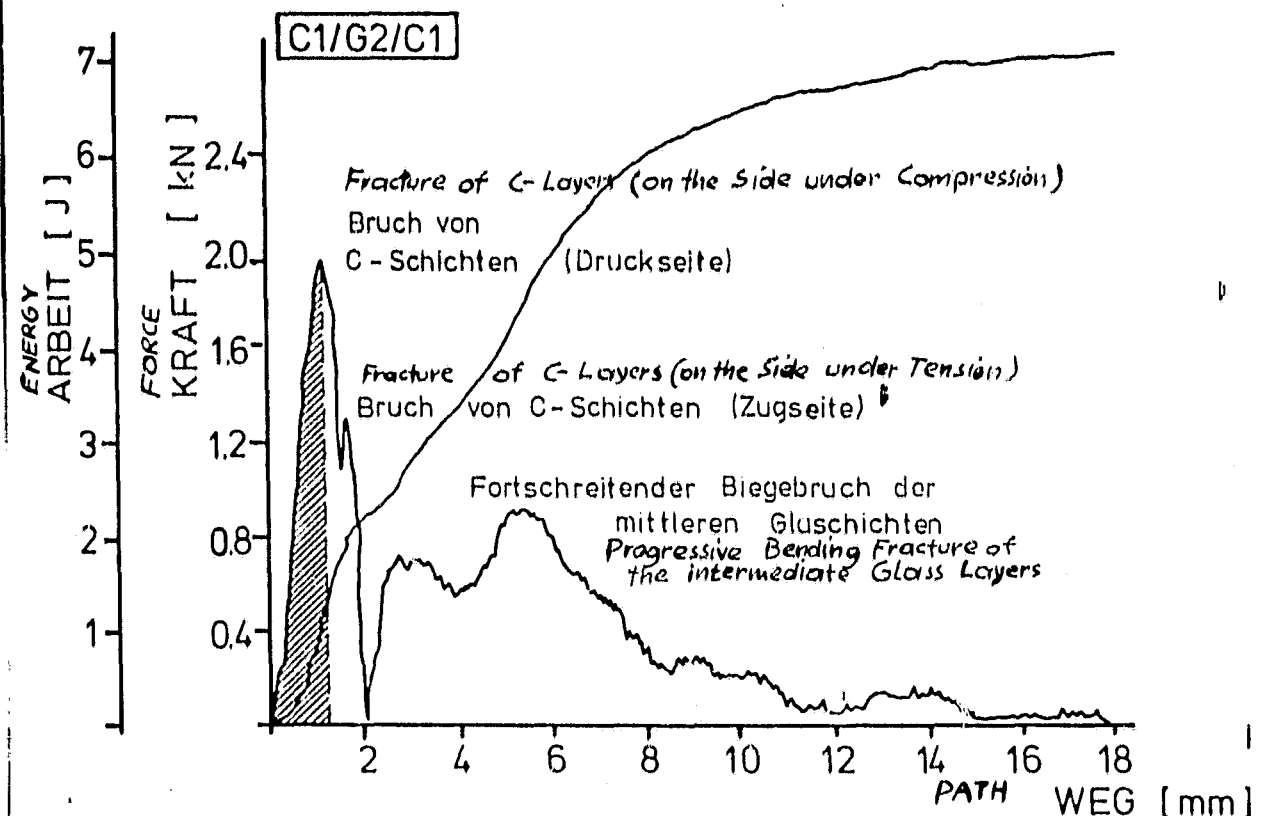
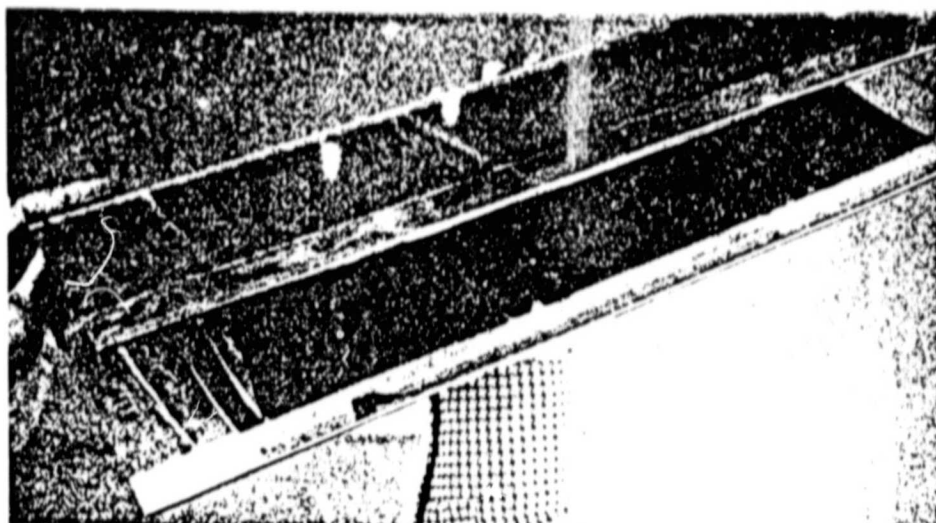
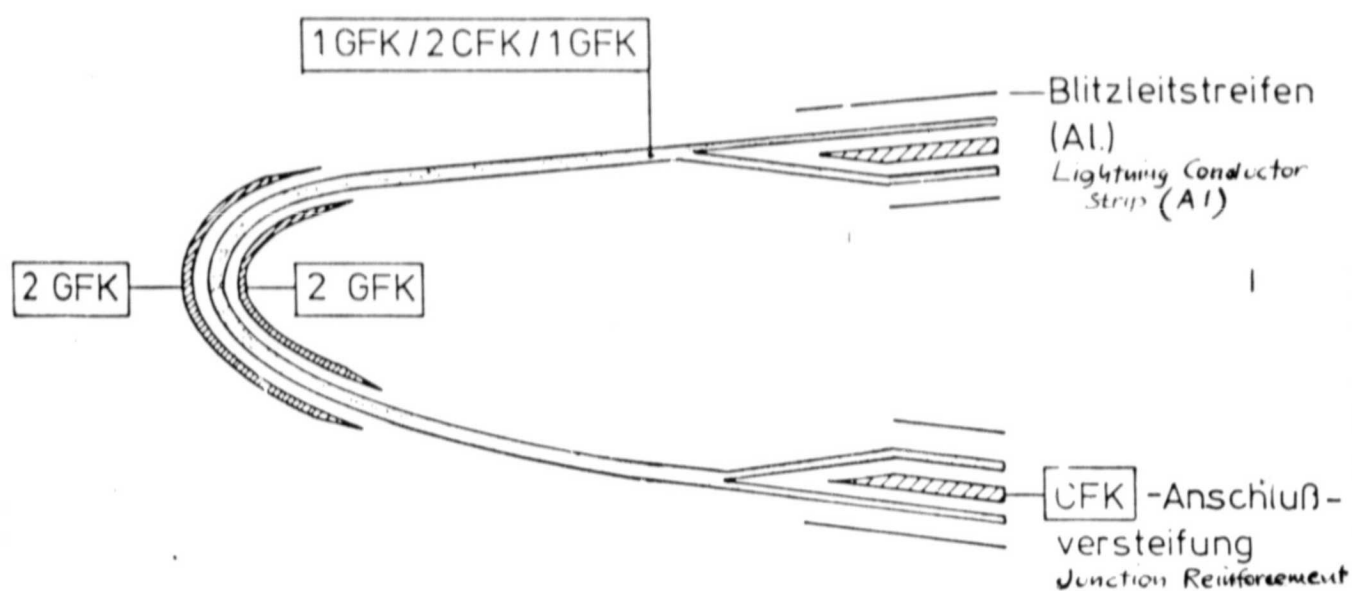


Fig. 2. Impact behavior for a blocked structure.



CFK - Rippen  
Ribs



MATERIAL:

Vicotex 1452 / G 803 CFK-Gew. / 664 GFK-Gew.

Preliminary Experiments with:

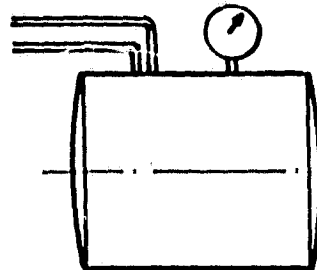
Vorversuche mit:

Code 69 / A 002 CFK-Gew. / 181 GFK-Gew.

Fibredux 920 / 916 / TS-5 CFK-UD / 181 GFK-Gew.

Fig. 3. Structural composition of the nose.

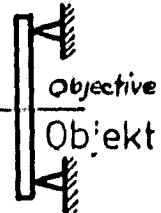
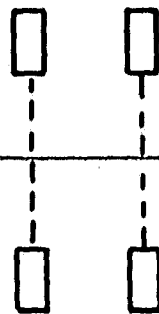
STONE DAMAGE  
STEINSCHLAG 50 m/s



Luftdruck - Kanone  
Air Pressure - Cannon



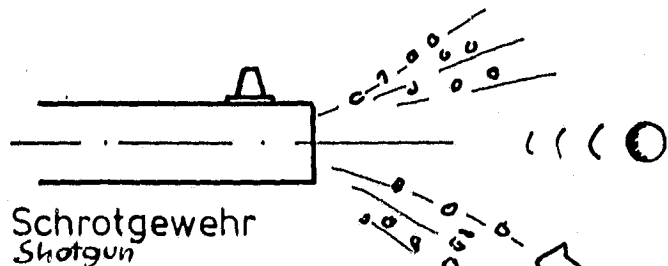
Light Barrier  
Lichtschranke



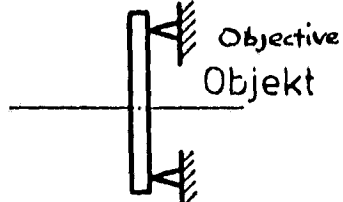
Kolben aus P.U.-Schaum  
(für verschiedene Geschoss - Ø )  
Piston, or P.U. - Foam  
(for different projectile diameters)

Steuerung der Geschwindigkeit durch Kesseldruck  
Control of Velocity through Boiler Pressure

HAIL STONE DAMAGE  
HAGELSCHLAG 250 m/s



Schrotgewehr  
Shotgun



Patrone  
Cartridge

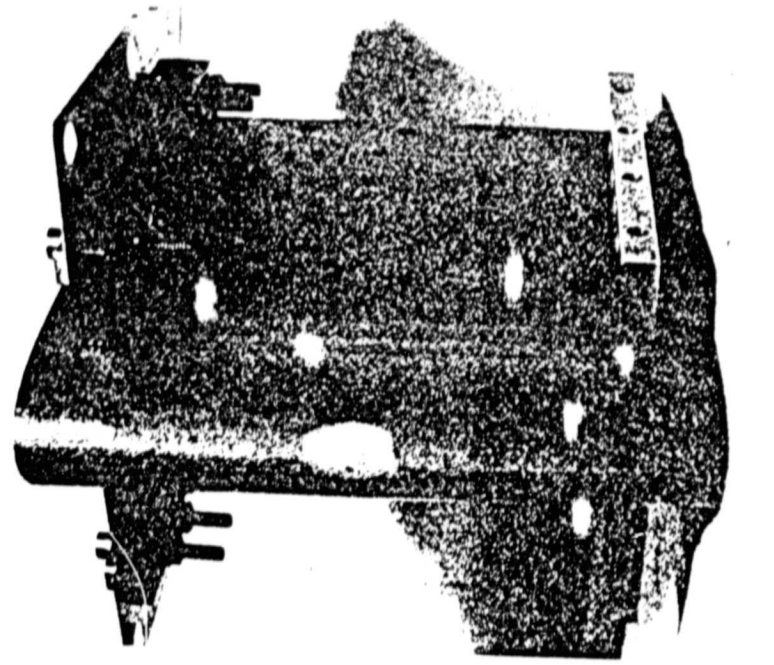


Eiskugel (15 mm Ø)  
Ice Bullet

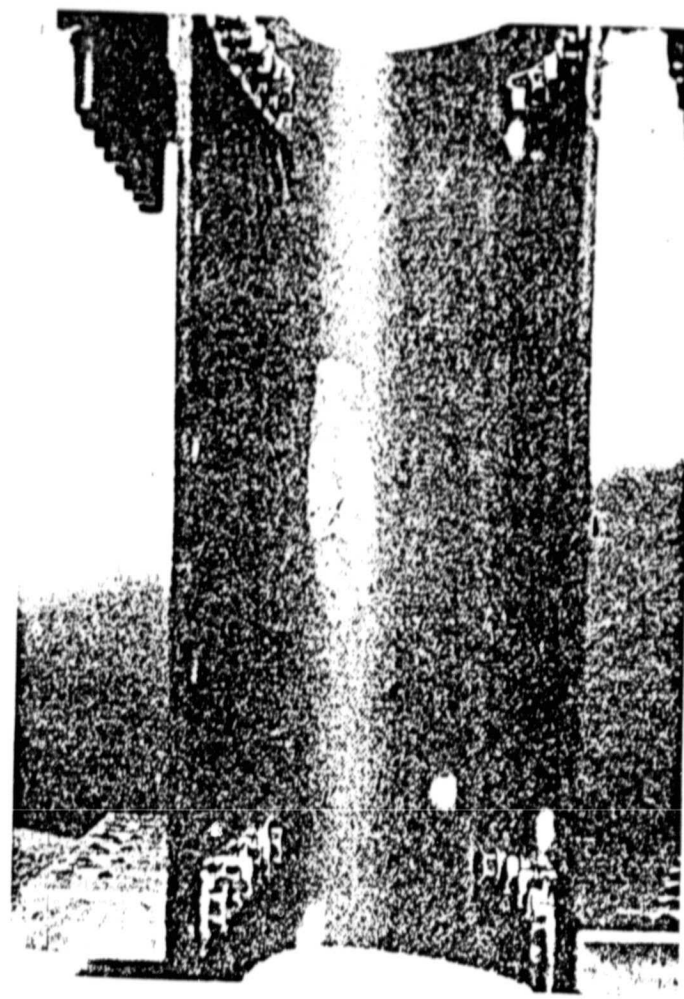
Styrofoamzylinder  
disintegrates after leaving the Muzzle  
zerplatzt nach Verlassen der Mündung

Steuerung der Geschwindigkeit durch Pulvermenge  
Control of Velocity through Quantity of Powder

Fig. 4. Simulation of damage through stones and hailstones.

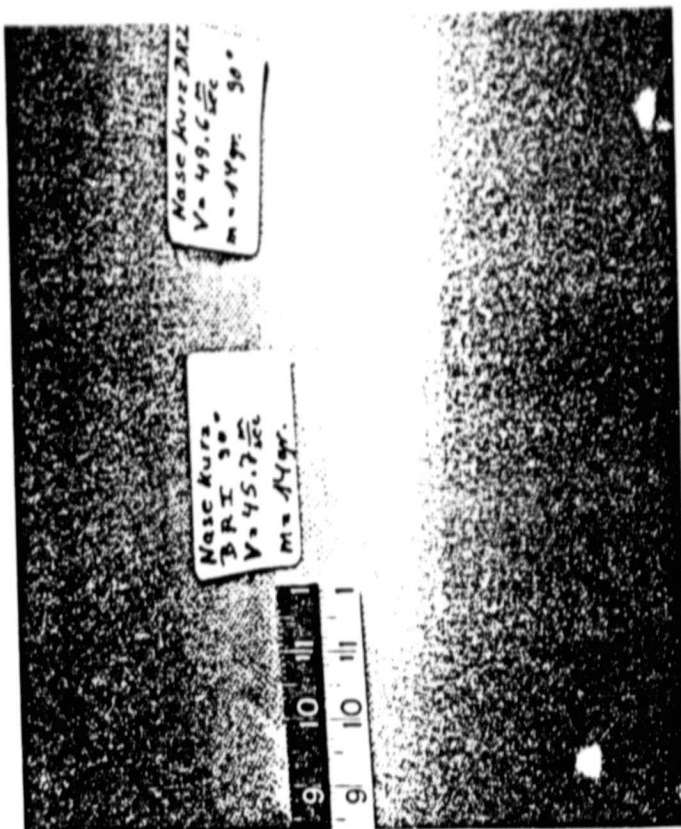


a) Vorderseite  
*Front*

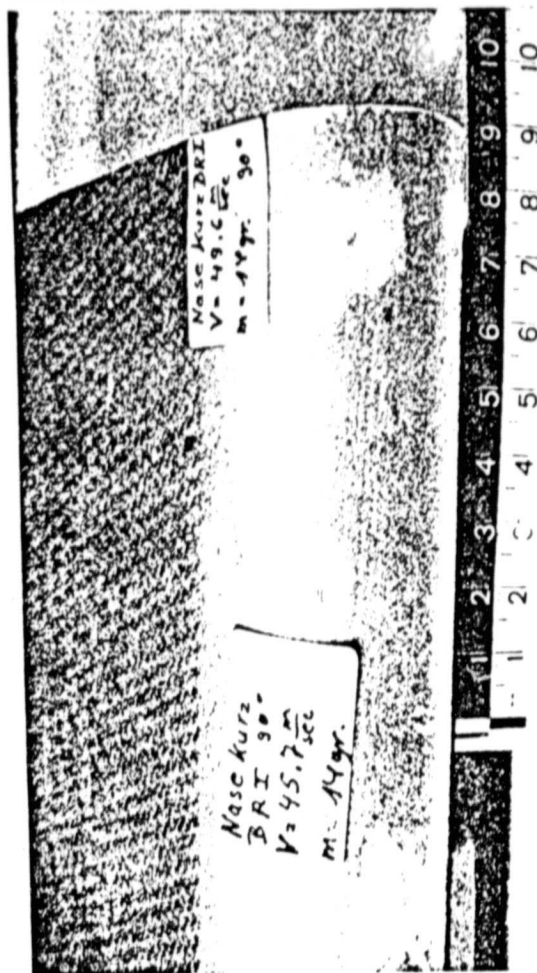


b) Rückseite  
*Back*

Fig. 5. Experimental nose section (Code 69) with stone damage.



a) Vorderseite  
*Front*



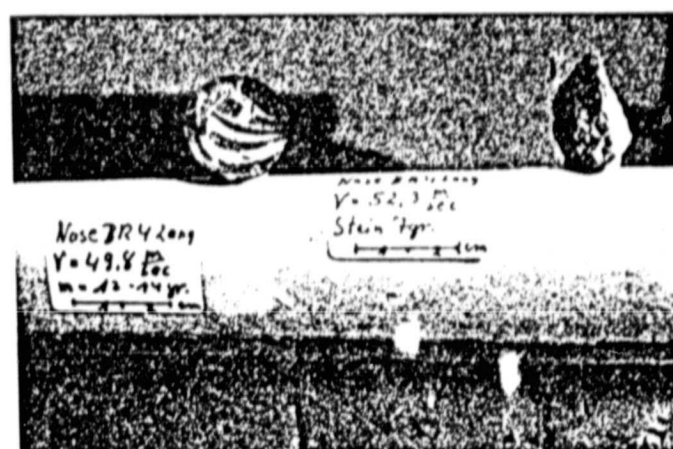
b) Rückseite  
*Back*

REPRODUCIBILITY OF THE  
ORIGINAL PAGE IS POOR

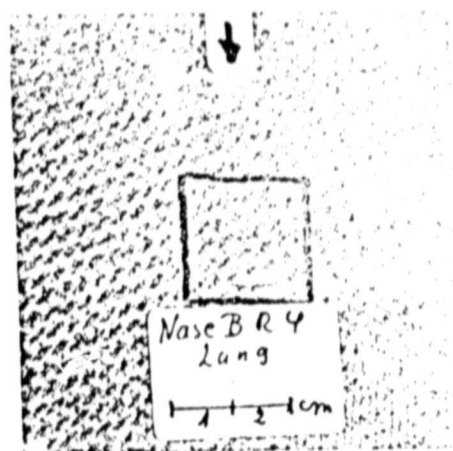
Fig. 6. Experimental nose section (Vicotex 1452) with stone damage).

REPRODUCIBILITY OF THE  
ORIGINAL PAGE IS POOR

Stone Projectiles for  
Simulation of Stone  
Damage

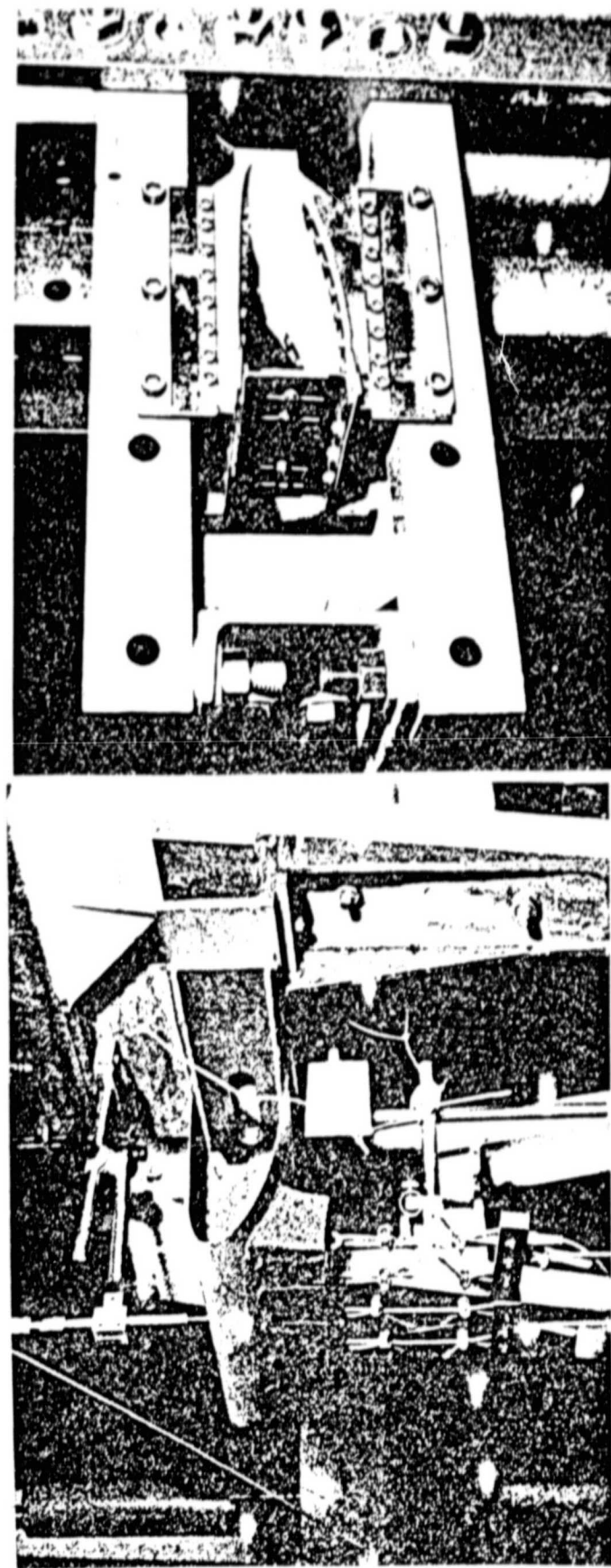


Experimental  
Nose-Section with  
Damage after  
Bombardment with  
Glassy Bullets and Stones



Damage on the Side of the Nose  
(Vicotex 1452) by impact of  
a Screwdriver from a Height  
of 1.8 m with a mass of 115 g

Fig. 7. Impact tests on fiber composite--noses.



Luftlastbiegung  
Air pressure Bending

Torsion / Biegung  
Torsion / Bending

Fig. 8. Experimental arrangement.

REPRODUCIBILITY OF THE  
ORIGINAL PAGE IS POOR

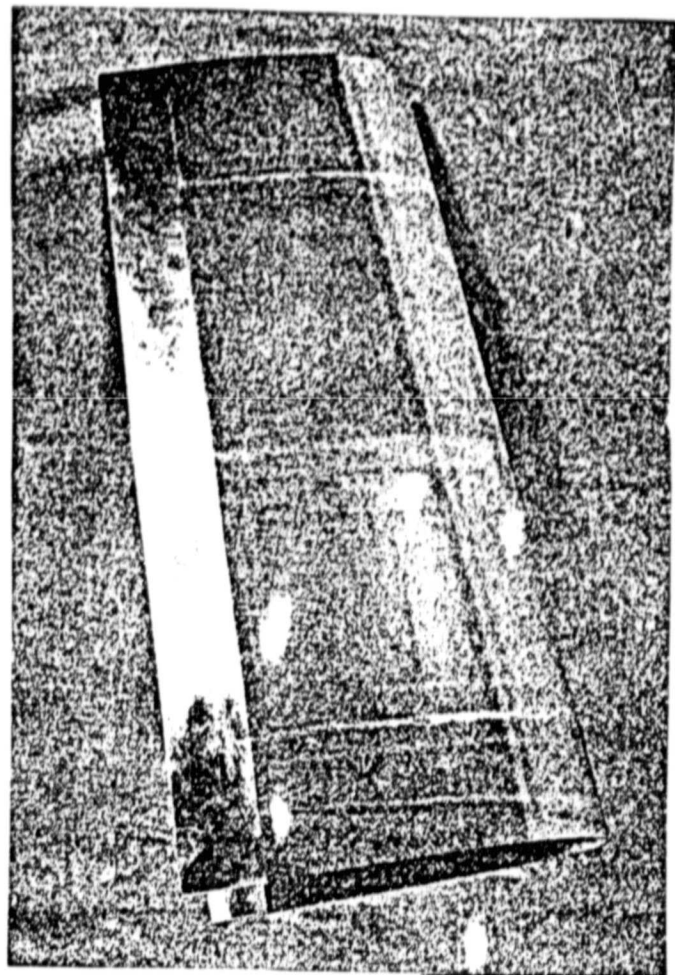


Fig. 9. Nose section as composite structure.

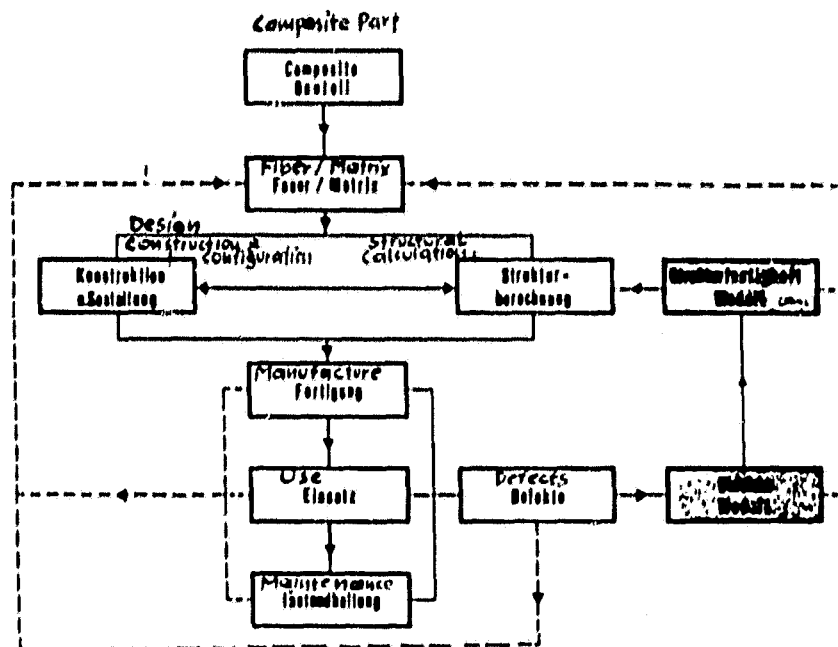


Fig. 10. Rough sketch of various phases of a composite structure. The models for field defects and structural strength for fiber-reinforced materials are only in the development stage.

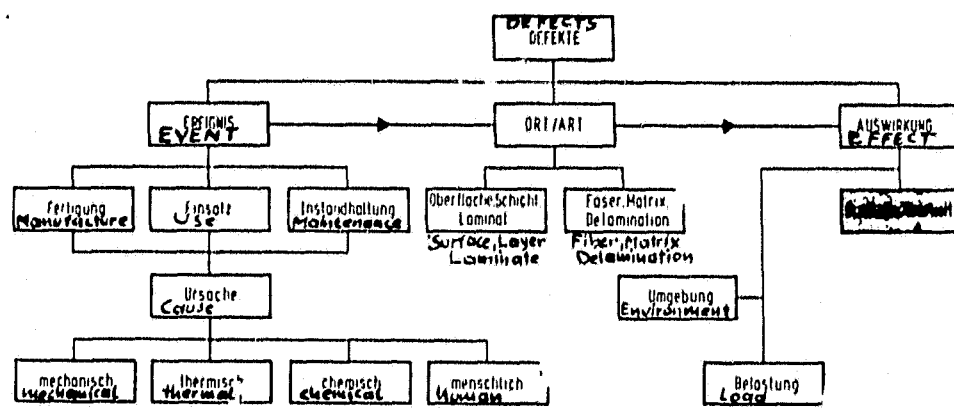


Fig. 11. Fault tree for classification of defects that can occur in composite structures.

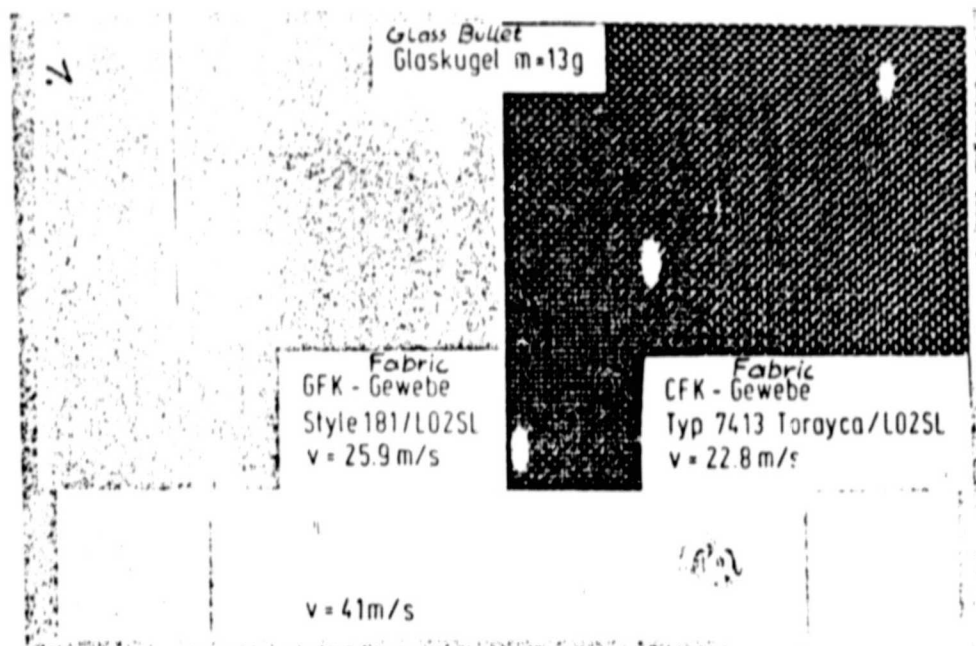
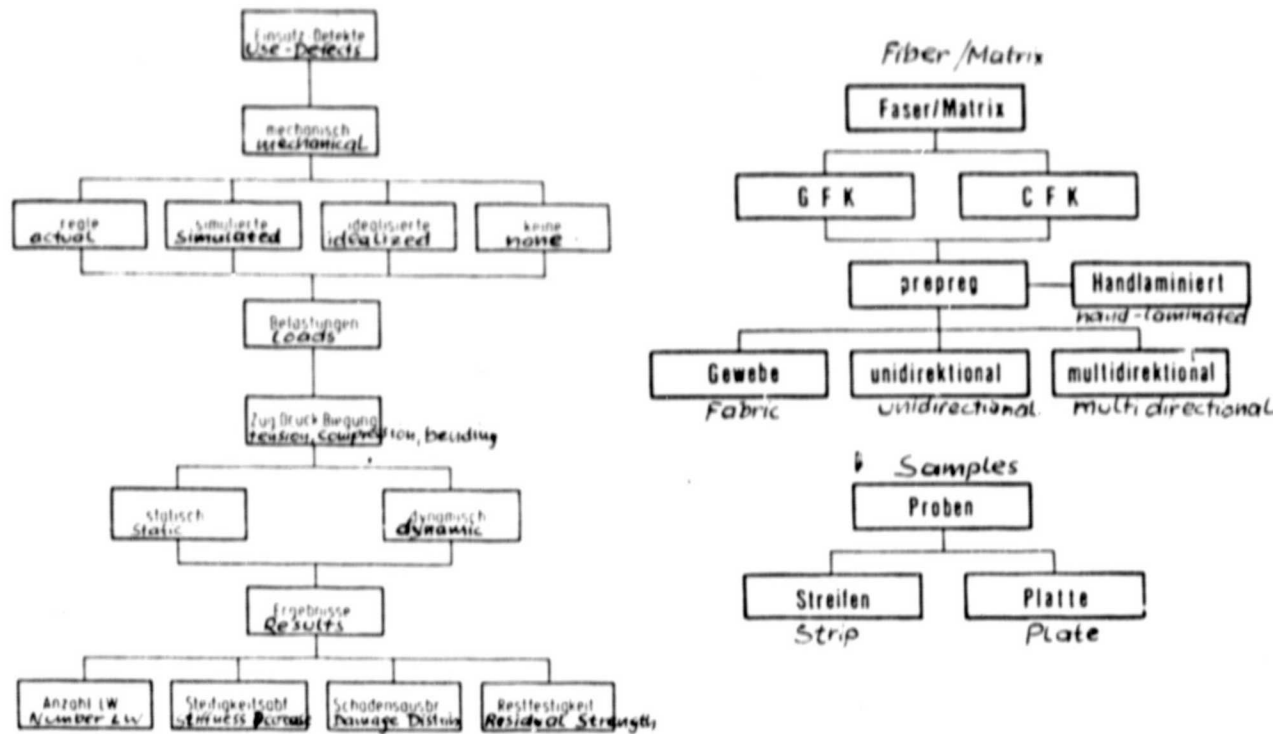


Fig. 12. Program survey 1BK detects and their effects.

REPRODUCIBILITY OF THE  
ORIGINAL PAGE IS POOR

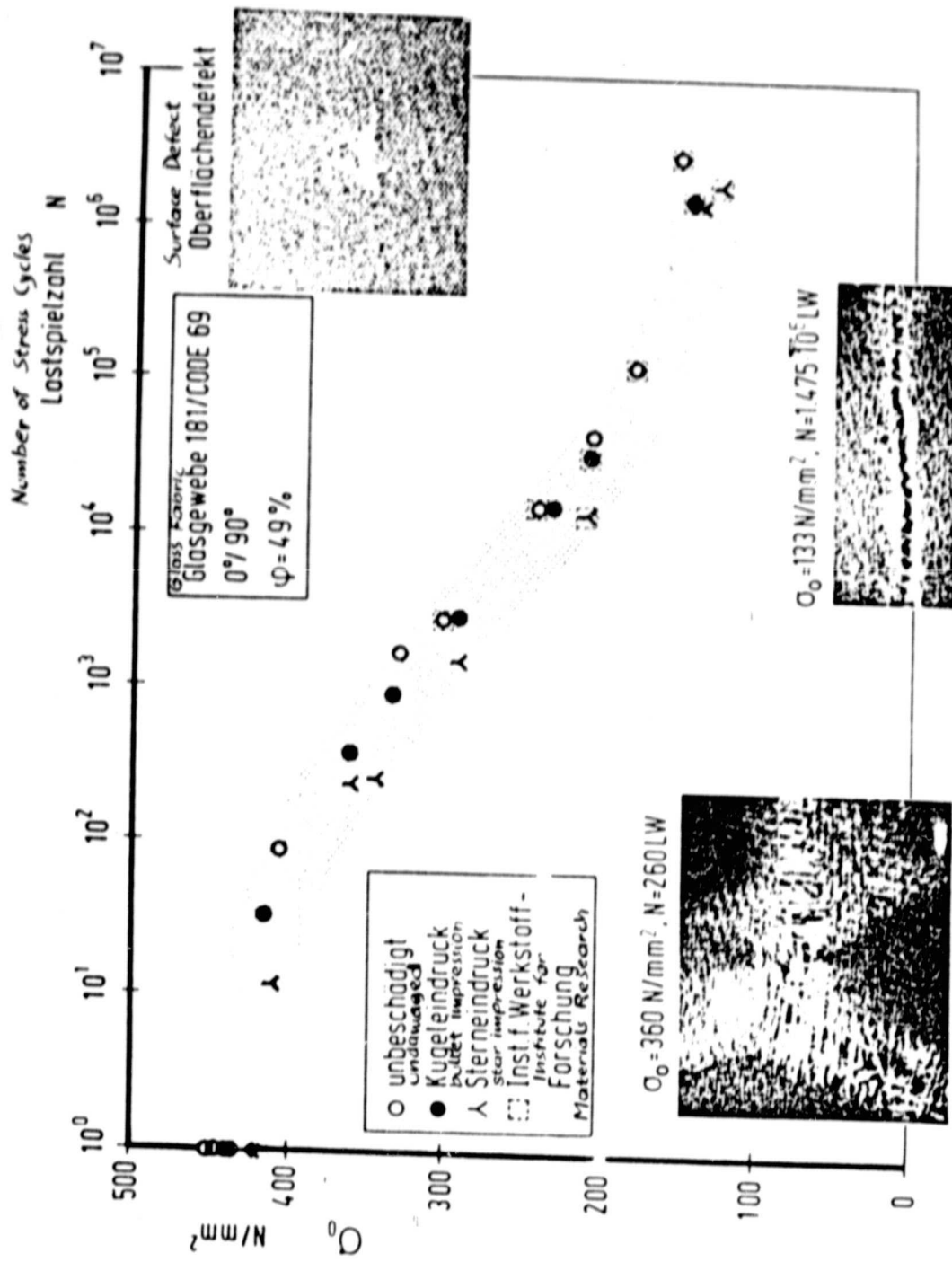
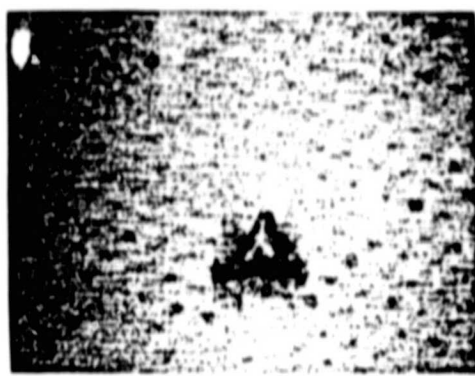
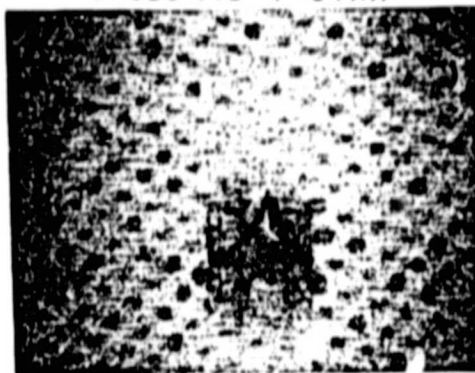


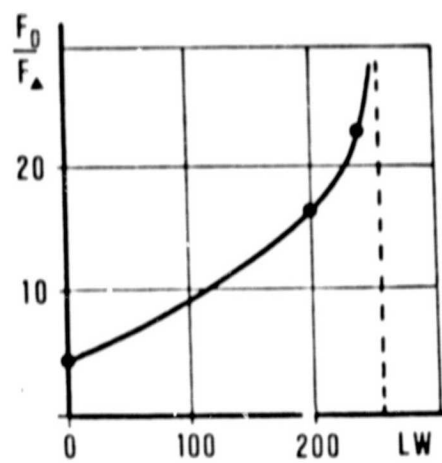
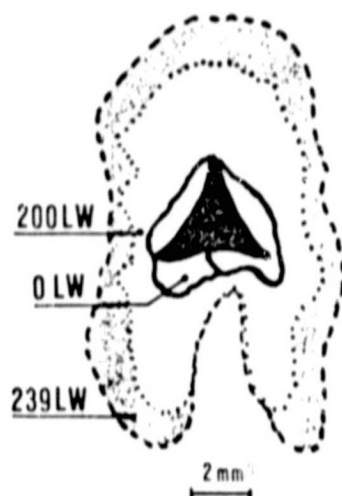
Fig. 13. Wöhler Curve--tensile stress of varying magnitude.



Sample  
Probe 14D  $P=34\text{ kN}$

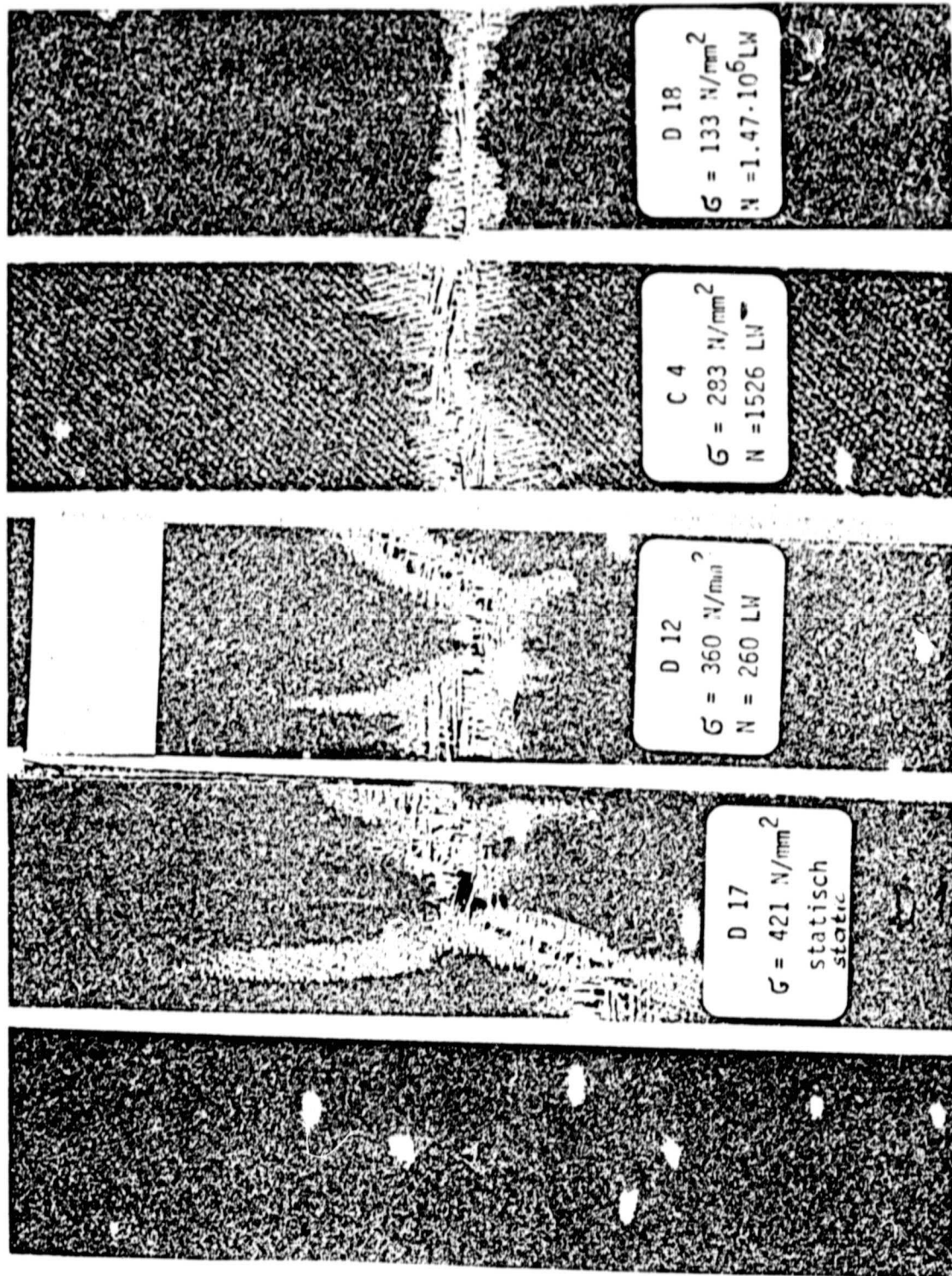


$P=34\text{ kN}$ ,  $N=120\text{ LW}$   
Sample  
Probe D12



Delaminationsfortschritt in Abhängigkeit der Lastwechselzahl  
Zugschwellbelastung ( $P_0=30\text{ kN}$ , GFK-Gew.  $0^\circ/90^\circ$ )  
Progress of Damage as Function of the Number of Stress Cycles of the  
Tensile Stress of variable Magnitude ( $P_0=30\text{ kN}$ , GFK-Gew.  $0^\circ/90^\circ$ )

Fig. 14. Progress of damage.



REPRODUCIBILITY OF THE  
ORIGINAL PAGE IS POOR

Fig. 15. Types of failure of GFK-0/90- - fabric samples.

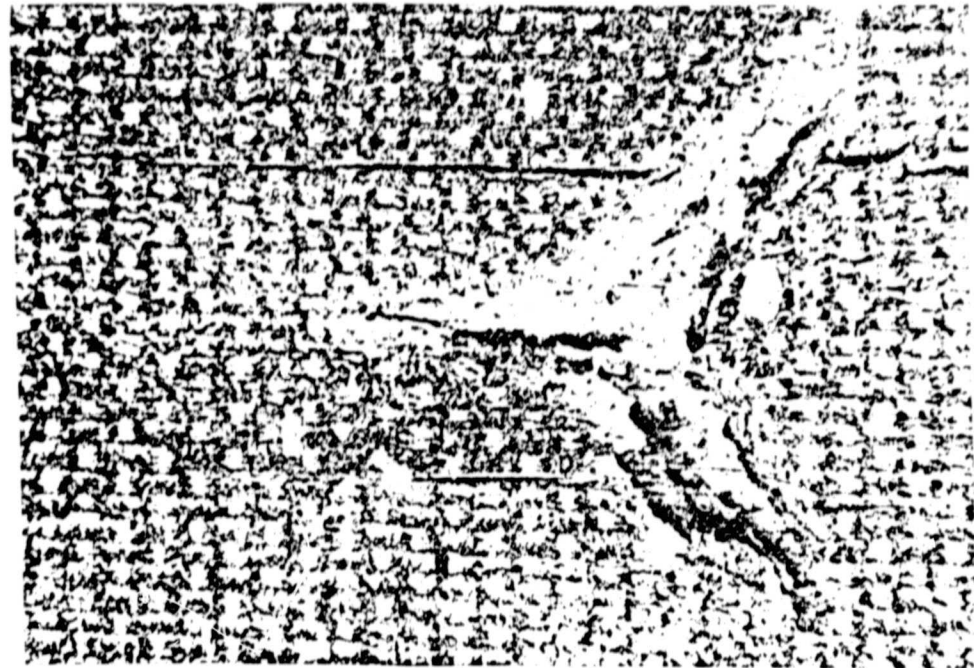
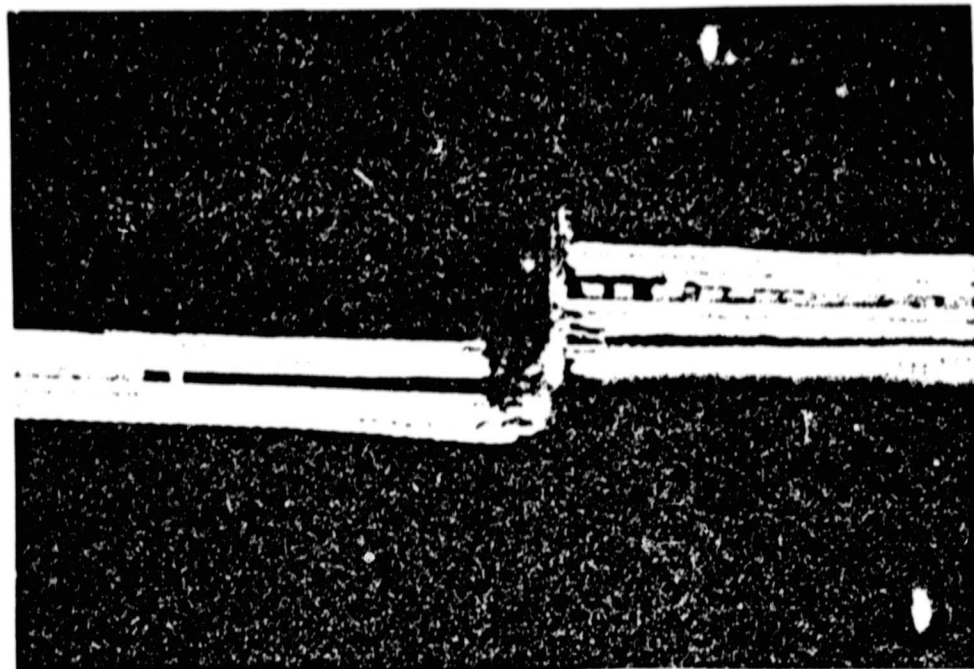


Fig. 16. CFK-T 300/Code 69--[0/90] 3S.

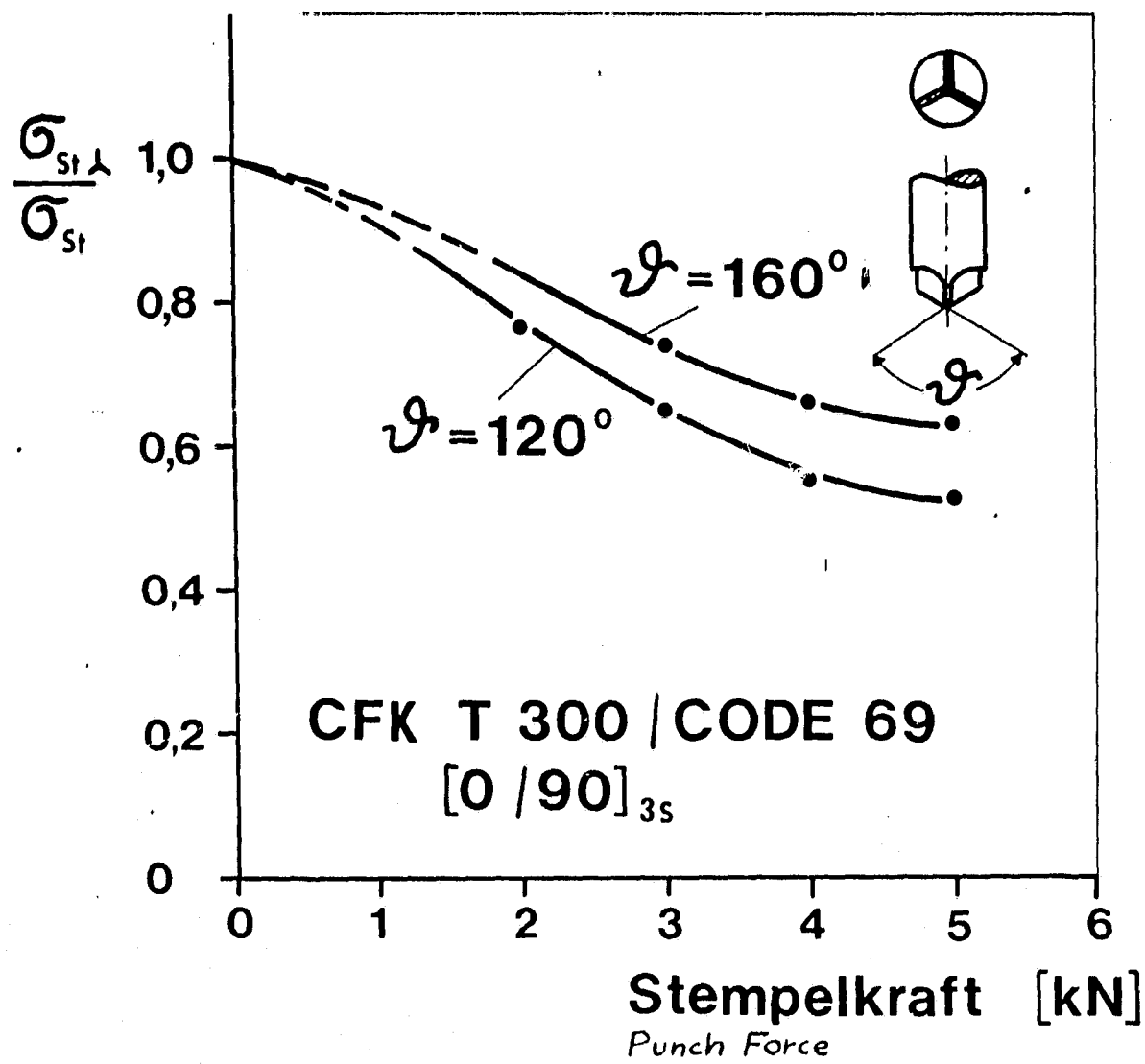


Fig. 17. Influence of damage parameters.

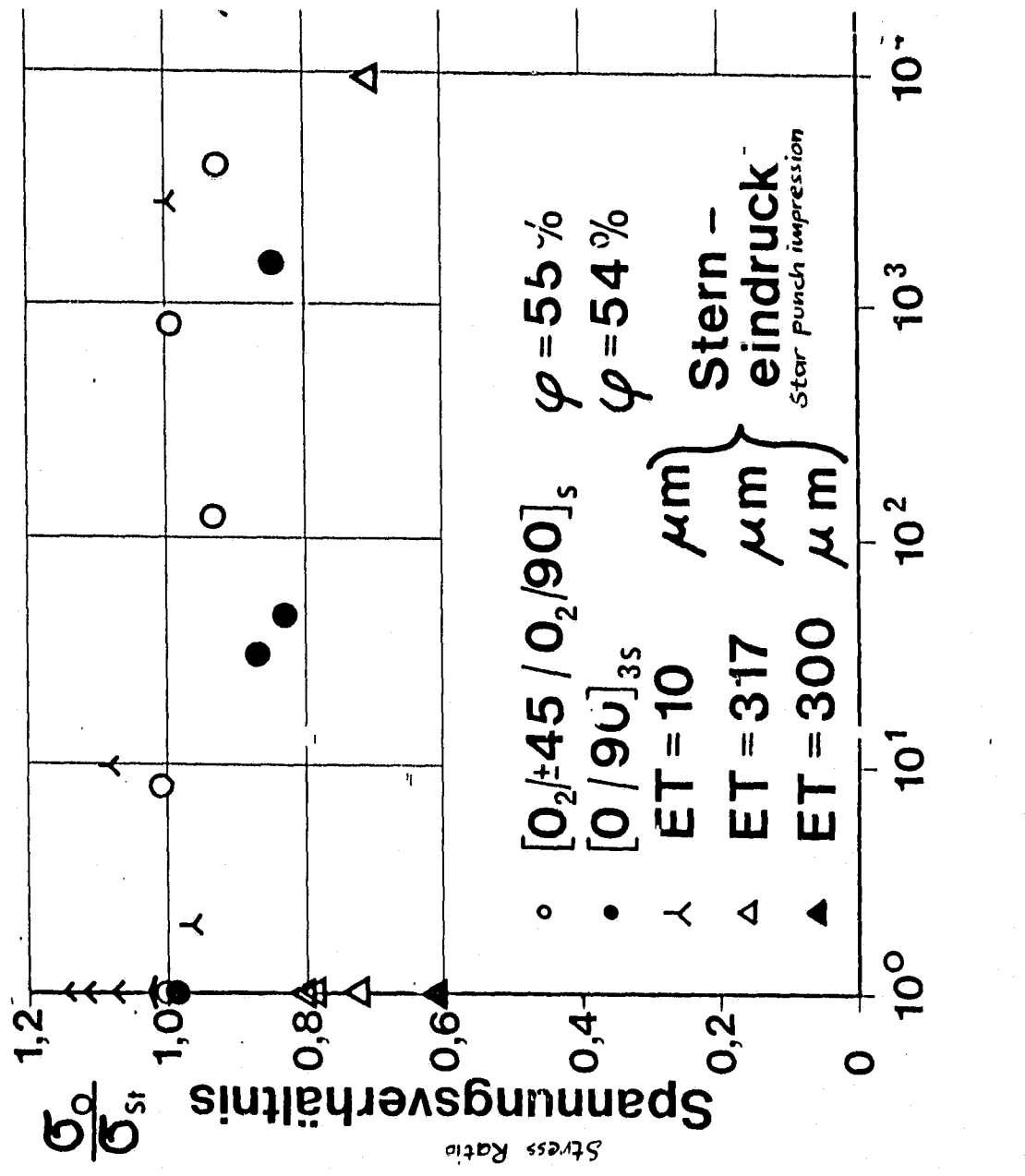


Fig. 18. Behavior of T300/Code 69 under tensile stress of varying magnitude.

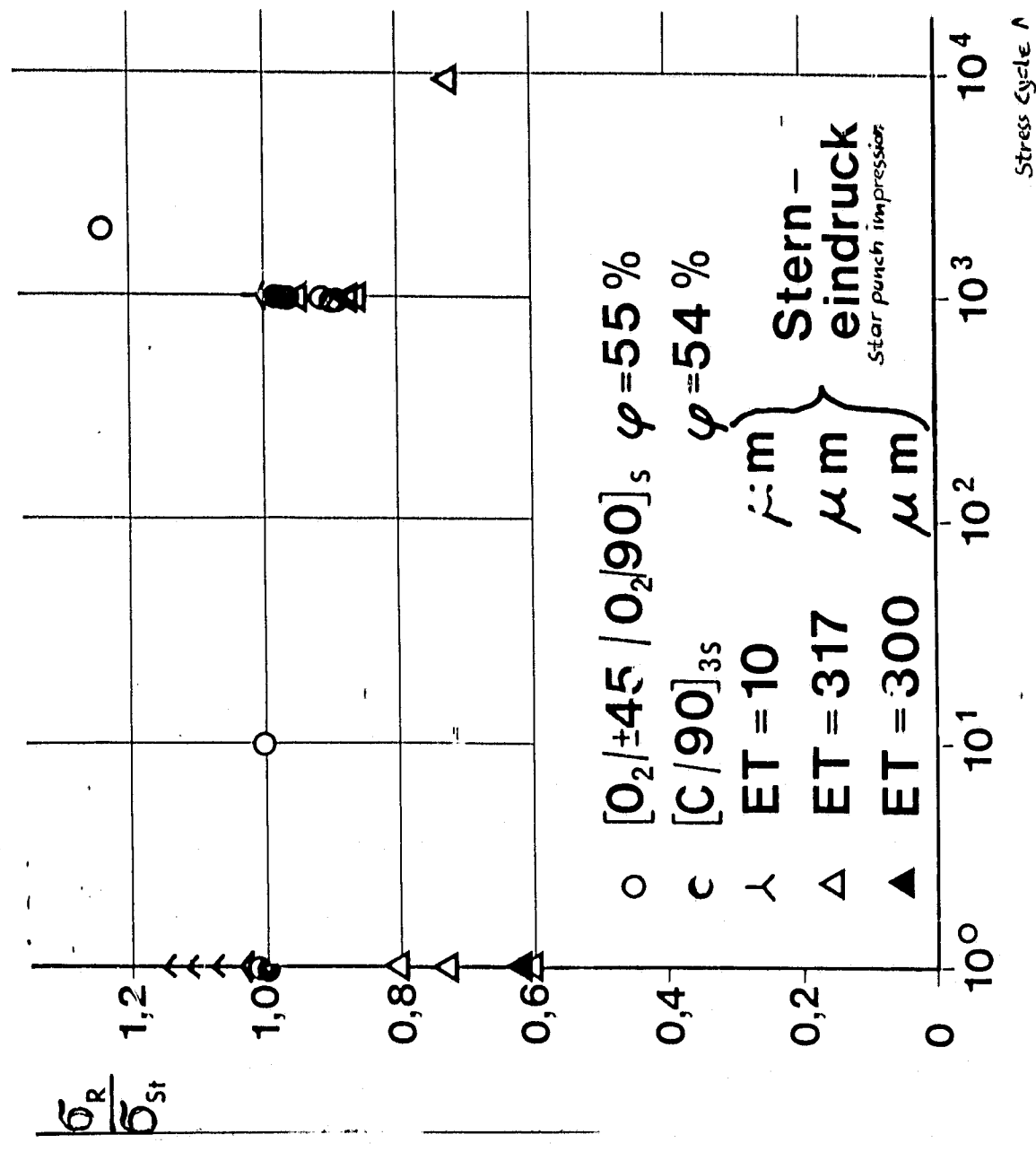


Fig. 19. Residual strength of T300/Code 69 after subjection to tensile stress of varying magnitude.

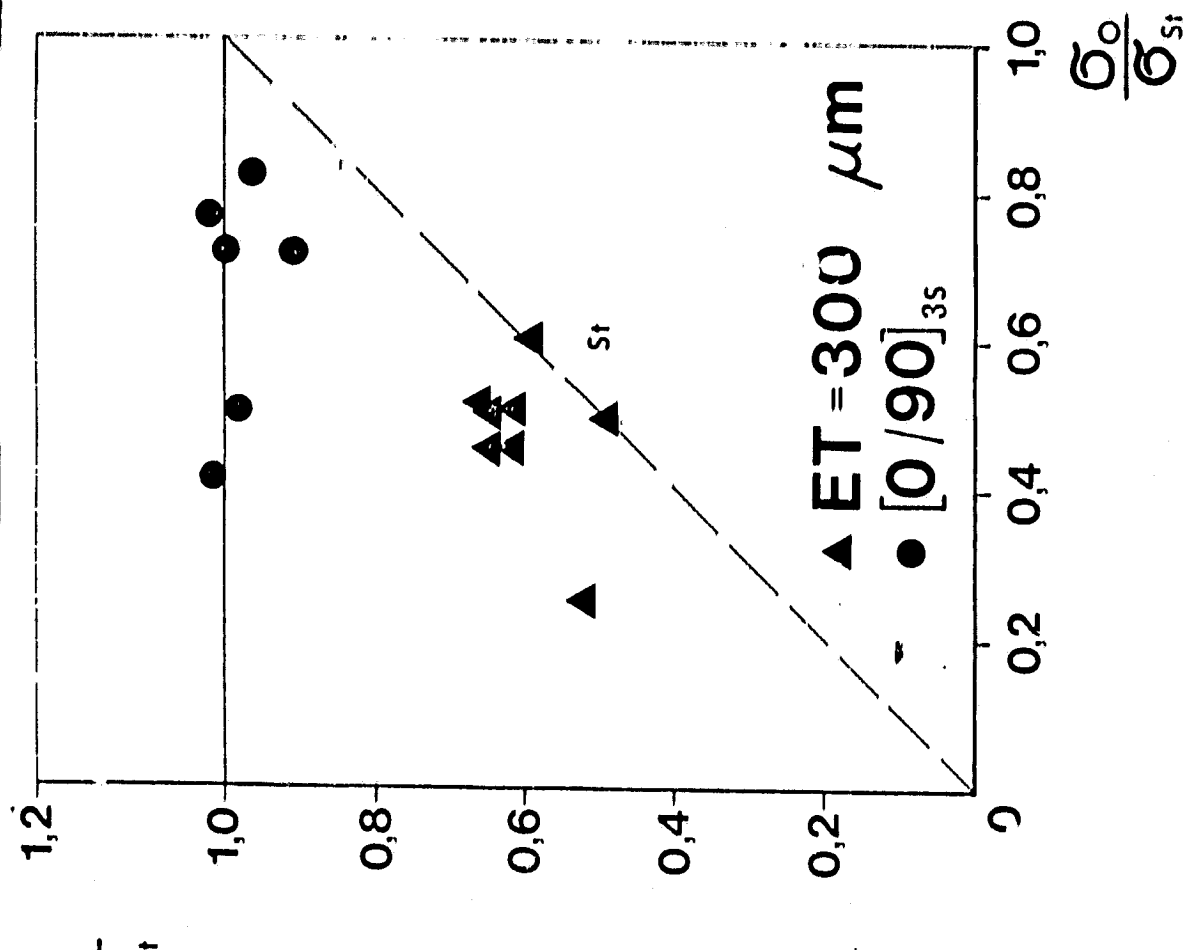
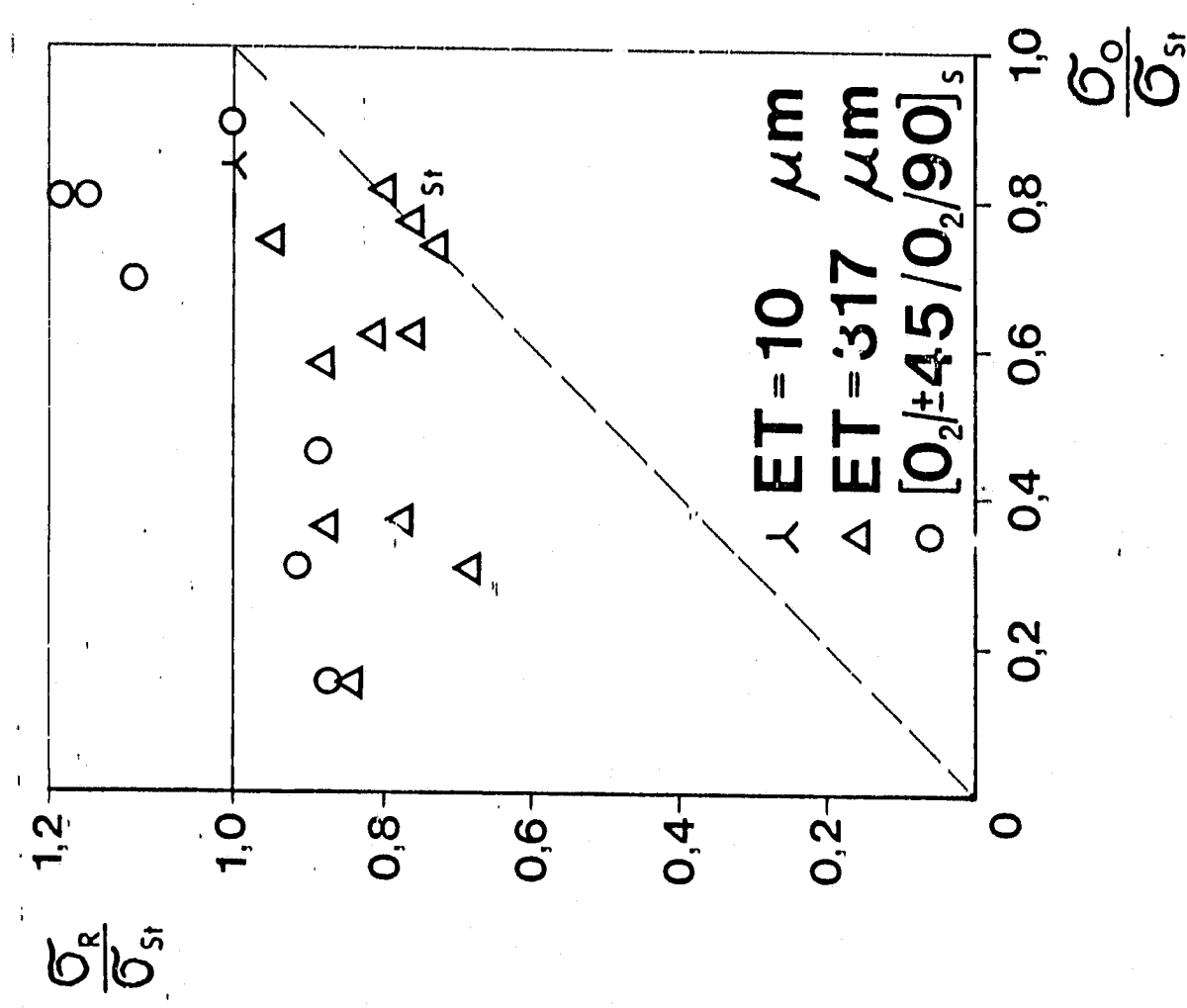


Fig. 20. Influence of tensile stress of varying magnitude on the residual strength of T300/Code 69.